

Data-independent Acquisition Improves Quantitative Cross-linking Mass Spectrometry

Authors

Fränze Müller, Lars Kolbowski, Oliver M. Bernhardt, Lukas Reiter, and Juri Rappsilber

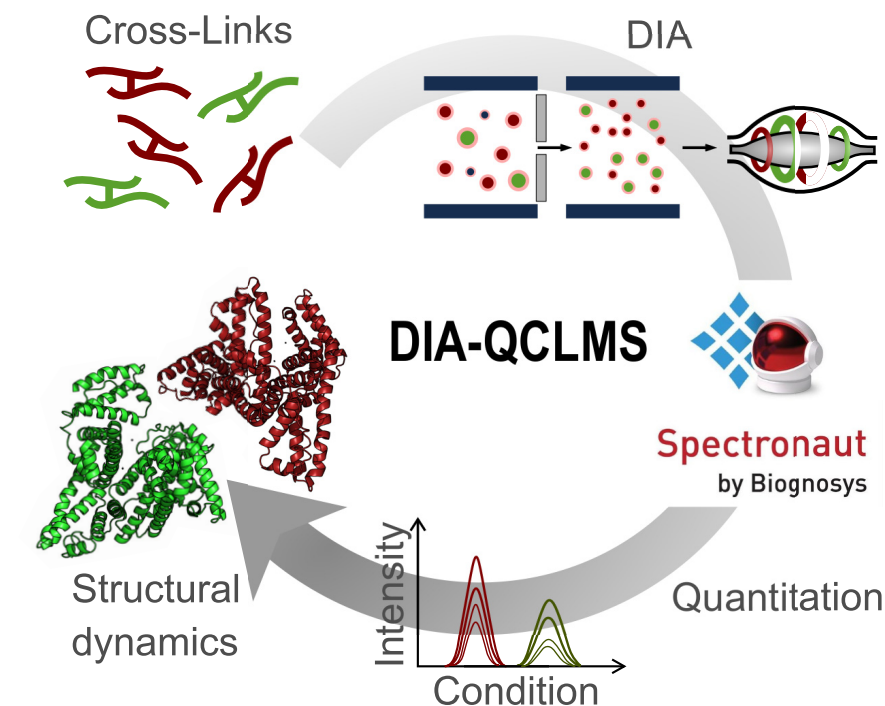
Correspondence

juri.rappsilber@tu-berlin.de

In Brief

We present here a simple, user friendly and automated new quantitative cross-linking mass spectrometry (QCLMS) workflow comprising data-independent acquisition (DIA) for acquiring mass spectrometry data and Spectronaut, one of the leading DIA analysis tools. DIA cross-linking data outperforms DDA in reproducibility and accuracy of quantitation results. DIA-QCLMS tolerates complex backgrounds and through its automation recommends itself for routine application in the analysis of protein complex dynamics.

Graphical Abstract



Highlights

- Quantitative cross-linking mass spectrometry (QCLMS) was automated by Spectronaut.
- Data-independent acquisition (DIA) was adapted to QCLMS.
- Accuracy and precision of quantitation improves with DIA over DDA.
- QCLMS is now ready for use in complex samples.



Data-independent Acquisition Improves Quantitative Cross-linking Mass Spectrometry*

✉ Fränze Müller‡, ✉ Lars Kolbowski‡§, ✉ Oliver M. Bernhardt¶, Lukas Reiter¶, and ✉ Juri Rappsilber‡§||

Quantitative cross-linking mass spectrometry (QCLMS) reveals structural detail on altered protein states in solution. On its way to becoming a routine technology, QCLMS could benefit from data-independent acquisition (DIA), which generally enables greater reproducibility than data-dependent acquisition (DDA) and increased throughput over targeted methods. Therefore, here we introduce DIA to QCLMS by extending a widely used DIA software, Spectronaut, to also accommodate cross-link data. A mixture of seven proteins cross-linked with bis[sulfosuccinimidyl] suberate (BS³) was used to evaluate this workflow. Out of the 414 identified unique residue pairs, 292 (70%) were quantifiable across triplicates with a coefficient of variation (CV) of 10%, with manual correction of peak selection and boundaries for PSMs in the lower quartile of individual CV values. This compares favorably to DDA where we quantified cross-links across triplicates with a CV of 66%, for a single protein. We found DIA-QCLMS to be capable of detecting changing abundances of cross-linked peptides in complex mixtures, despite the ratio compression encountered when increasing sample complexity through the addition of *E. coli* cell lysate as matrix. In conclusion, the DIA software Spectronaut can now be used in cross-linking and DIA is indeed able to improve QCLMS. *Molecular & Cellular Proteomics* 18: 786–795, 2019. DOI: 10.1074/mcp.TIR118.001276.

Cross-linking mass spectrometry (CLMS)¹ is a powerful tool for studying the 3D structure of proteins and their complexes (1–5). Chemical cross-linking helps to identify residue pairs that are in proximity in native structures but not necessarily in primary sequence, by introducing covalent bonds between these residues. Subsequent to the cross-linking reaction and the proteolytic digestion of proteins, cross-linked peptides can be enriched (using strong cation exchange (SCX) (6) or size exclusion chromatography (SEC) (7), for example) and

then identified through liquid chromatography-mass spectrometry (LC-MS) combined with database searching.

Although a protein's function links to its three-dimensional structure, these structures are intrinsically dynamic and can change (8, 9). Adding quantitative information to the relative abundances of cross-linked residue pairs offers a unique opportunity to study the structural flexibility and changes of proteins (10). Previous studies using quantitative cross-linking mass spectrometry (QCLMS) have provided concepts and techniques for studying changing protein states including activation (11), regulation of protein networks (12–15), maturation of complexes (16), regulation of enzyme activity (17–19), protein-protein interactions (20, 21) and interactome analysis of cancer cell lines (22).

Broadly speaking, two quantitative strategies are suitable for QCLMS: labeled and label-free. Although isotope-labeled cross-linkers (23) are commonly used in labeling strategies (13, 14, 16–19, 24–29), other general strategies have also been adapted to QCLMS including SILAC (stable isotope-labeled amino acids) (22, 30, 31) and isobaric labeling by TMT (32, 33) or iTRAQ (34). In contrast, label-free quantitation (LFQ) might allow for a simpler experimental design and reduced costs. Importantly, although samples are processed separately during LFQ experiments, which may increase technical variance, label-free QCLMS is as reproducible as other proteomic techniques (35).

Multiple approaches are used in proteomics for LFQ (36, 37). Data-dependent acquisition (DDA) unfortunately results in poor reproducibility for low abundance proteins or peptides (38–40) and therefore is not ideal for the typically low abundance cross-linked peptides. Targeted proteomic strategies such as SRM (MRM) or PRM excel for less abundant peptides (41–45). Early targeted approaches on cross-linking mass spectrometry using an inclusion list were performed by Barysz *et al.* 2015 (46) and more recently, on MS2 level using parallel reaction monitoring (PRM) and Skyline (47). However, the

From the ‡Bioanalytics, Institute of Biotechnology, Technische Universität Berlin, 13355 Berlin, Germany; §Wellcome Centre for Cell Biology, School of Biological Sciences, University of Edinburgh, Edinburgh EH9 3BF, Scotland, United Kingdom; ¶Biognosys, 8952 Zürich-Schlieren, Switzerland

✂ Author's Choice—Final version open access under the terms of the Creative Commons CC-BY license.

Received December 12, 2018

Published, MCP Papers in Press, January 16, 2019, DOI 10.1074/mcp.TIR118.001276

number of targets is limited, and the analysis is demanding. Data-independent acquisition (DIA) promises a solution to all these challenges by requiring minimal assay development and allowing large scale quantitative analysis with high reproducibility (48, 49). This has not yet been exploited in QCLMS because of current software restrictions regarding cross-linked peptides.

In recent years, significant advances in software for both CLMS and QCLMS have propelled the cross-linking field forward, enabling a deeper understanding of dynamic protein systems and a wider range of workflows (50). Here, we developed a DIA-QCLMS workflow that uses the Spectronaut software for the quantitation of observed unique residue pairs. We determined the accuracy and reproducibility of our DIA-QCLMS workflow at both MS1 as well as MS2 level, using a mix of seven proteins, each cross-linked using bis[sulfosuccinimidyl] suberate (BS³), and *E. coli* cell lysate as matrix.

EXPERIMENTAL PROCEDURES

Reagents—The seven-protein mix comprised human serum albumin (HSA), cytochrome C (bovine heart), ovotransferrin (Conalbumin, chicken egg white), myoglobin (equine heart), lysozyme C (chicken egg white), and catalase (bovine liver), all purchased individually from Sigma Aldrich (St. Louis, MO). Creatine kinase Type M (rabbit muscle) was purchased from Roche (Basel, Switzerland). The cross-linker BS³ was purchased from Thermo Scientific Pierce (Rockford, IL).

Cross-linking Reaction—Cross-linking reactions of the individual proteins were performed in parallel as previously described (35). In short, purified proteins were mixed separately with BS³ (1 $\mu\text{g}/\mu\text{l}$ protein concentration), with a protein to cross-linker mass ratio of 1:4. After incubation on ice, the reaction was stopped using saturated ammonium bicarbonate. Cross-linked proteins were subjected to SDS-PAGE, visualized using Coomassie staining and monomer bands were excised for digestion.

Sample Preparation—Cross-link protein gel bands were reduced, alkylated and digested using trypsin as described before (51). After digestion, peptides were extracted from gel bands using 80% v/v acetonitrile (ACN) and concentrated to a final ACN content of nominally 5% v/v using a Vacufuge Concentrator (Eppendorf, Germany). Tryptic peptides were enriched using strong cation exchange chromatography (SCX) as previously described (6) but using SCX-StageTips (52, 53) with minor modifications for activation of the Tip and gradient steps. The SCX-StageTips were activated using first methanol, following buffer 2 (0.5% AcH, 80% CAN), buffer 1 (0.5% AcH), high salt buffer (0.5% AcH, 20% CAN, 600 mM NH₄Ac) and

finally again buffer 1. Peptides were eluted in steps using: 50 mM NH₄Ac (fraction 1), 100 mM NH₄Ac (fraction 2), 200 mM NH₄Ac (fraction 3), 300 mM NH₄Ac (fraction 4), 500 mM NH₄Ac (fraction 5), 600 mM NH₄Ac (fraction 6). Peptides were then desalted using C₁₈-StageTips (52, 54) and eluted using 80% v/v ACN, 0.1% v/v TFA. Peptides were dried down and resuspended in 2% v/v ACN, 0.1% v/v formic acid (FA) to a final protein concentration of 0.75 $\mu\text{g}/\mu\text{l}$.

Data Acquisition—LC-MS/MS analysis was performed using a tribrid Orbitrap mass spectrometer (Orbitrap Fusion™ Lumos, Thermo Fisher Scientific, CA) with a “high/high” (high-resolution MS1 and MS2) acquisition strategy. 1.5 μg peptides were injected for data-dependent acquisition (DDA) experiments. For data-independent acquisition (DIA), the stock solution (1.5 μg peptides) was diluted to reach 0.1 \times , 0.3 \times , 0.5 \times , 0.7 \times , 0.9 \times , and 1 \times (undiluted). 1.5 μg tryptic *E. coli* cell lysate was added as matrix to each sample of the dilution series to assess DIA in the context of analyzing a complex sample. iRT peptides (Biognosys, Switzerland) were added to each sample before MS acquisition. The peptide separation was carried out on an EASY-Spray column (50 cm \times 75 μm ID, PepMap C₁₈, 2 μm particles, 100 Å pore size, Thermo Fisher Scientific, Germany). Peptides were separated using a 150 min gradient and analyzed in DDA mode as described before (35). In short, precursor ions were detected in the Orbitrap at 120K resolution using m/z range 400–1600. Ions with charge states from 3+ to 7+ were selected for fragmentation. Selected ions were isolated and fragmented by high energy collision dissociation (HCD) and detected in Orbitrap at 30K resolution (55). In DIA mode, precursor ions were acquired using a MS1 master scan (m/z range: 400–1200, max. injection time: 60 ms, AGC target: 4×10^5 , detector: Orbitrap, resolution: 60K), following 66 DIA scans for MS2 within a fragmentation range of m/z 120–1200 using an isolation window width of m/z 12 and a max. injection time of 50 ms. Selected ions were isolated in the quadrupole, fragmented using HCD (normalized collision energy 30%) and detected in Orbitrap at 30K resolution.

Identification of Cross-linked Peptides—The raw mass spectrometric data files were processed into peak lists using MaxQuant (56) (v. 1.5.0.0) as described previously (35). Xi (v. 1.6.723) (57) was used for database search. The database comprised the sequences of HSA (UniProt ID: P02768), cytochrome C (P62894), ovotransferrin (P02789), myoglobin (P68082), creatine kinase (P00563), lysozyme C (P00698), and catalase (P00432) and the reverse sequence of each of these proteins as decoys. Search parameters were: MS tolerance: 6 ppm, MS/MS tolerance: 20 ppm, enzyme: trypsin, missed cleavages: 4, cross-linker: BS³, fixed modification: carbamidomethylation of cysteine, variable modification: oxidation of methionine and modification by BS³ with the second NHS ester hydrolyzed or amidated, with BS³ reaction specificity at lysine, serine, threonine, tyrosine and N termini of proteins. In a cross-link analysis, the false discovery rate (FDR) can be calculated on different information levels: PSMs, peptide pairs, residue pairs (RPs) and protein pairs (58). We here considered residue-pair FDR, which were estimated using xiFDR (v 1.0.21.45) with the equation: $\text{FDR} = \text{TD-DD/TT}$ (58) and filtering to only use cross-link PSMs within proteins. The max. protein ambiguity was set to 1. Other settings were left on default. Identification with 5% FDR at link level were accepted for quantitation.

Creation of Spectral Library for Cross-links and Quantitation—Quantitation was performed on MS1 and MS2 level using Spectronaut (version 11.0.15038.23.25164) (59, 60). The spectral library of cross-linked peptides was introduced as a .csv file, following the standard format for custom libraries in Spectronaut (Manual for Spectronaut 11, available on Biognosis website). The .csv file was constructed from our DDA data using xiDIA-library (a Python script generated by us for this purpose). xiDIA-library is an open source collaborative initiative available in the GitHub repository <https://github.com/Rappsilber-Laboratory/xiDIA-library>. It is freely available

¹ The abbreviations used are: CLMS, cross-linking mass spectrometry; AcH, acetic acid; ACN, acetonitrile; AGC, automatic gain control; BS³, bis[sulfosuccinimidyl] suberate; CL, cross-linking; CV, coefficient of variation; DDA, data-dependent acquisition; DIA, data-independent acquisition; DTT, dithiothreitol; HCD, high energy collision dissociation; HAS, human serum albumin; IAA, 2-iodoacetamide; iTRAQ, isobaric tags for relative and absolute quantitation; LC-MS, liquid chromatography-mass spectrometry; LFQ, label-free quantitation; NH₄Ac, ammonium acetate; PRM, parallel reaction monitoring; PSM, peptide spectrum matches; QCLMS, quantitative cross-linking mass spectrometry; SCX, strong cation exchange chromatography; SILAC, stable isotope-labelled amino acids; SRM/MRM, selected reaction monitoring/multiple reaction monitoring; TMT, tandem mass tag; URPs, unique residue pairs.

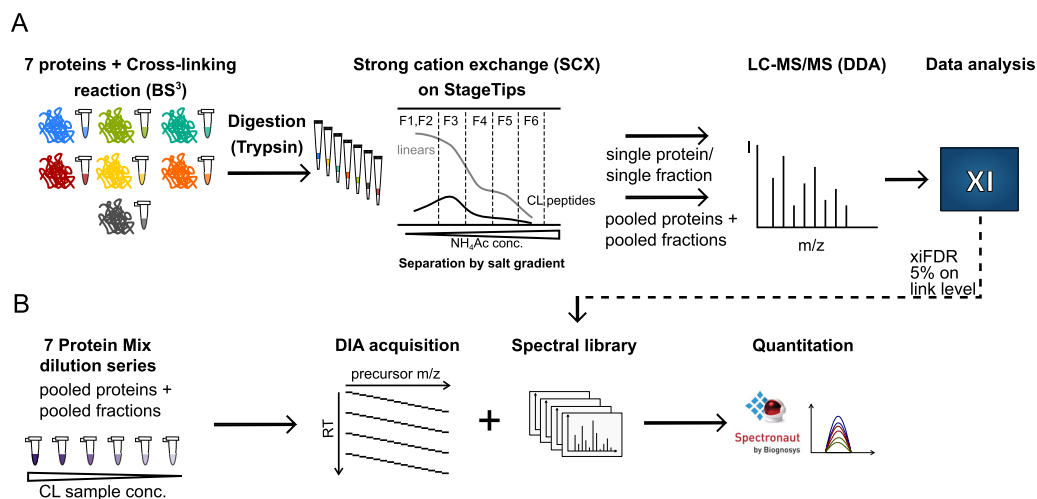


FIG. 1. Label-free DIA-based cross-linking quantitation workflow. *A*, Sample preparation workflow using SCX chromatography to fractionate cross-linked peptides. *B*, Cross-link identification and quantitation workflow using Xi Software for identification and Spectronaut for quantitation.

under the Apache License v2.0. xiDIA-library extracts the required information for the spectrum library from different sources: Precursor information (for example, m/z , charge) are read from the xiFDR PSM result file; fragment data is obtained through annotation by xiAnnotator [<https://github.com/Rappsilber-Laboratory/xiAnnotator>]; retention times are extracted from mzML files, obtained by subjecting raw files to MSconvert (61); iRT values are determined using linear regression of observed retention times of iRT peptides. Up to 10 cross-link containing fragments and up to 10 linear ones were chosen from the highest intensity b- or y-ion signals in the m/z range 300–1400. The library was imported as an external library, leaving out the Prepare Perspective option in Spectronaut (called Library in Spectronaut 12). Note, for optimal import use the “set up a DIA Analysis from File” option in the View tab (Analysis tab in Spectronaut 12) and follow the wizard. Spectronaut 11 and Spectronaut 12 show the same performance in analyzing cross-linking data (see supplemental Fig. S1).

Protein modifications must be defined in Spectronaut to enable internal decoy generation for quantitation. The following cross-linker modifications were added manually to the default list of modifications in Spectronaut: BS³-OH (156.078 Da), BS³-NH₂ (155.094 Da), and BS³-d0 (138.068 Da). Defaults were used for the remaining settings. MS1 and MS2 filtering was done according to the Spectronaut manual with the following deviations: Quantitation tab: Interference correction unticked, Minor (Peptide) Grouping: by modified sequence, Major Group Top N unticked, Minor Group Top N ticket (max 10, min 1), Minor Group Quantity: mean precursor quantity. Note that the interference correction in Spectronaut works only for complex mixtures with a background proteome library (linear peptides). Interference correction requires matching sequences from the spectral library to the FASTA file supplied for the analysis. This is currently not possible with cross-linked peptides. After automated peak-picking and retention time alignment of Spectronaut, a manual correction of peak boundaries was performed for cross-linked peptides with a coefficient of variation (CV) above 30% using the filter option “condition CV” in the View Perspective. Data from Spectronaut was exported using the Report Perspective into a .xls file to integrate feature-level quantitation data into residue-level data using a standard spreadsheet application (Excel, Microsoft).

The background *E. coli* Library (linear peptides) was generated using MaxQuant for linear search with default settings and the Prepare Perspective option in Spectronaut (default setting).

Unfortunately it is not possible to use Spectronaut to perform DDA quantitation analysis, hence we had to use Skyline (62) (v. 4.2) to compare DIA and DDA quantitation results. Creation of Spectral library and quantitation settings in Skyline are as described previously (35). Shortly, the .ssl file for custom libraries in Skyline was constructed using an in-house-script based on peptide spectrum matches (PSM) of identified cross-linked peptides. The library file and the assigned mzML files are used to create the final spectral library within Skyline. The following modifications had to be defined in Skyline: cross-linker (25.968 Da), BS³-OH (156.078 Da), BS³-NH₂ (155.094 Da) and BS³-loop (138.068 Da), linkage site (1.0078 Da). The Spectral library is used to match precursor information to identified precursors to the DDA data. Note that quantitation in Skyline can currently only be performed on MS1 level for many targets. After quantitation, the data were exported into a .csv file and feature-level data were integrated into residue-level using Excel. CV values within replicates (triplicates) had to be calculated separately for each unique residue pair using the following equation: $c_v = \sigma/\mu$.

Experimental Design and Statistical Rationale—For DIA MS experiments, we analyzed triplicates of a pooled seven-protein mixture in a dilution series of 0.1×, 0.3×, 0.5×, 0.7×, 0.9×, and 1× stock solution. Each dilution was injected three times, resulting in 18 LC-MS injections (DDA: 15 injections, missing 0.7×). A second dilution series of the same steps as before was mixed with tryptic *E. coli* cell lysate as matrix and injected as described above. Hence, 36 individual DIA runs were analyzed in total for this study. Peak areas were quantified in Spectronaut and Skyline. Conducting a dilution series prevented the mean peak intensity in the samples to be used for data normalization. Thus, nonnormalized data was used. Only cross-linked peptides quantified in three out of three technical replicas (triplicates) were considered for label-free quantitation. Statistical testing was performed using Spectronaut with default settings for statistical tests. A q value of 0.01 was used for filtering the results. The peak selection and boundaries of cross-linked peptides above a CV value of 30% was corrected manually (this applied to approximately one in four PSMs). It should be noted that the peak selection and boundaries in the DDA data were not corrected manually.

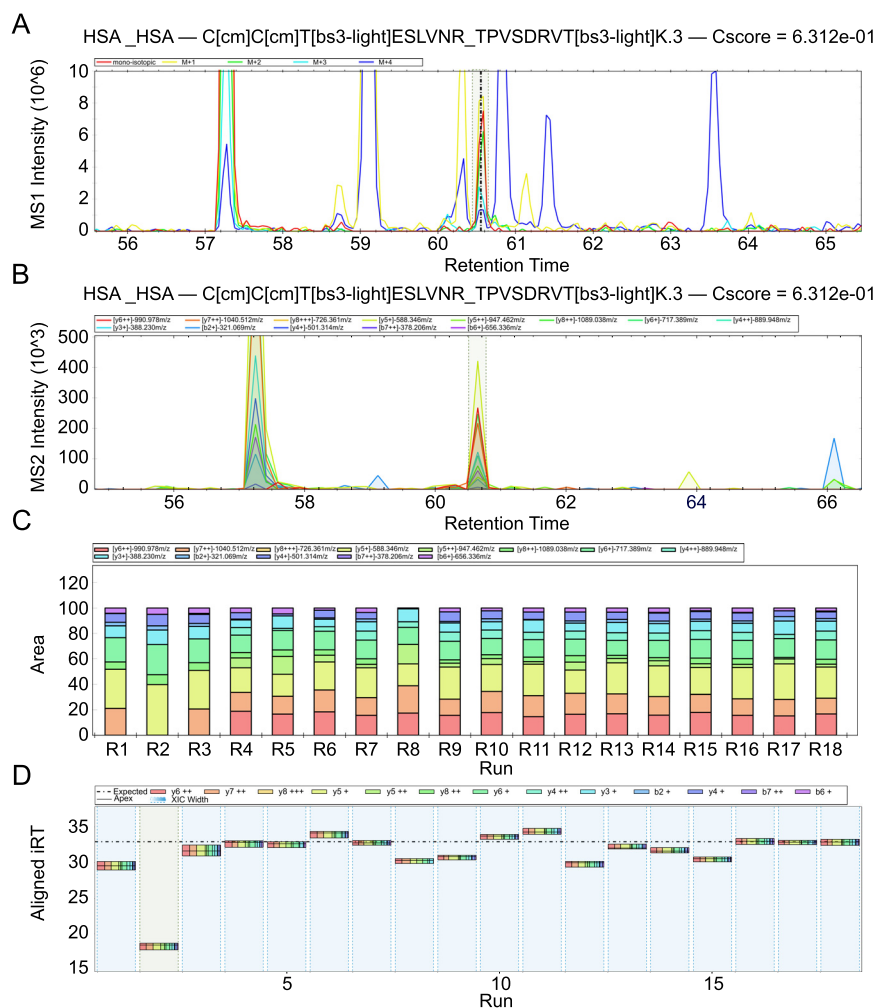


FIG. 2. Visualization of cross-linking features in Spectronaut software. A, MS1 isotope envelope XIC plot, showing extracted precursor ions M (red), M+1 (yellow), M+2 (green), M+3 (light blue), M+4 (dark blue). B, MS2 XIC plot, showing extracted fragment ion chromatograms in different colors. C, MS2 intensity alignment plot, showing normalized fragment intensities across all replica. D, Cross run RT accuracy plot, showing retention time comparison between all replica.

RESULTS AND DISCUSSION

Construction of Spectral Library—First, using data-dependent acquisition (DDA), we generated a library of fragmentation spectra for data-independent acquisition (DIA) analysis. Our sample comprised seven proteins (HSA, cytochrome C, ovotransferrin, myoglobin, creatine kinase, lysozyme, and catalase), each cross-linked separately in solution using BS³. We prevented cross-links between proteins from entering our analysis and retained the option to evaluate our identified cross-links against available 3D structures of the seven proteins by only exercising protein monomer SDS-PAGE bands for trypsin digestion. We fractionated and enriched the cross-link peptides of each protein into six SCX-StageTip fractions (6, 52). Each fraction was analyzed individually (totaling 49 runs) and pooled across all proteins and fractions (12 runs) by LC-MS using a “high-high” (high-resolution MS1 and MS2) strategy and DDA (Fig. 1A). The analysis yielded 414 unique residue pairs (URPs) across all seven proteins at 5% link level

FDR, compared with 83 URPs as seen previously (63). Of the 414 URPs, all were covered by crystallographic protein models, with 350 falling below 30 Å, and 64 (15%) above. The long-distance links did not distribute equally among the seven proteins. For example, in HSA (66 kDa, 137 links), we observed 6% long-distance links whereas we encountered 23% in the similar-sized ovotransferrin (76 kDa, 177 links). This indicates conformational flexibility rather than false identifications as the cause of the relatively high fraction of long-distance links. To further increase the library size, we included a public data set from our laboratory (PXD008550), which was generated using size exclusion chromatography with the same seven proteins, cross-linker, and protease. This added 121 URPs to the library including 16 long-distance links and thus did not change the overall match to the structures. We consider cross-linking at K, S, T, Y and protein N termini. 270 URPs included at least one S, T, or Y whereas 265 URPs included only K or N termini (1 URP). The spectral library was

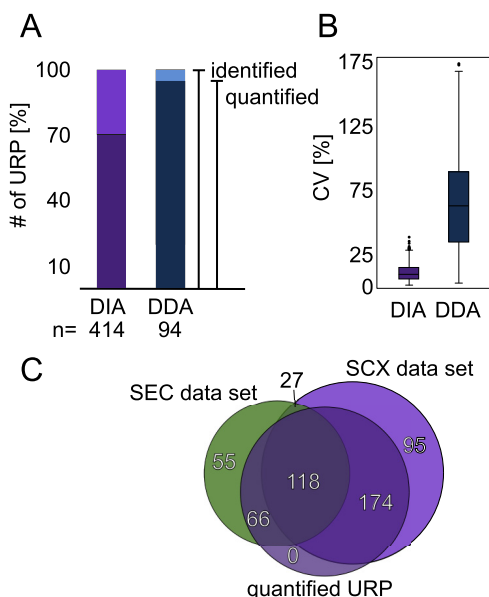


FIG. 3. Reproducibility of identification and quantitation of unique residue pairs (URPs). A, Comparison of DIA (violet) versus DDA (blue) acquisition in terms of identified (light color) and quantified (dark color) unique residue pairs in triplicates. B, Comparison of DIA (light purple) and DDA (blue) in terms of CV values of peak areas. Box plot whiskers extend 1.5 times the interquartile range. C, Venn diagram of unique residue pairs from SCX data set compared with a foreign SEC data set and quantified residue pairs.

then generated using xiDIA-library (see Experimental Procedures) and comprised 535 URPs, 2344 precursors and 34531 fragments in total. Our raw data, peak files and results files are accessible in the ProteomeXchange (64) Consortium via the PRIDE (65) partner repository with the data set identifier PXD011036.

Label-free Quantitation of Cross-linked Peptides by Spectronaut Using Data-Independent Acquisition—To assess the reproducibility of data-independent acquisition quantitation, we used the pooled sample of proteins and fractions for a dilution series experiment at 0.1 \times , 0.3 \times , 0.5 \times , 0.7 \times , 0.9 \times , and 1 \times of the stock mixture (Fig. 1B). iRT peptides were added to all samples to be used as the internal standard for retention time alignment in Spectronaut. Our DIA method (see Experimental Procedures) resulted in a cycle time of 5 s, leading to 14 data points per MS1 peak and 4 data points in MS2, on average. The low number of MS2 data points is caused by the small window size (m/z 12), that may limit the accuracy of our analysis in MS2. However, the small window size also reduces interferences by co-eluting precursors and hence increases sensitivity for low abundant cross-linked peptides. Analyzing cross-link DIA data required several changes to Spectronaut. The parsing rules were expanded to use cross-link specific information noted in the peptide comments column and the output file was expanded by an URP column (called “FG_Comment”). The work also required several software adjustments to be made (see release notes for

Spectronaut version 11.0.15038.23.25164). Spectronaut then successfully read in the cross-link DIA data, conducted retention time alignment and extracted precursor and fragment information based on the external spectral library (Fig. 2). Data was filtered to a q value of 0.01 (comparable to 1% FDR) (66–68). We manually inspected and corrected peak boundaries for all precursor and fragment species with a coefficient of variation (CV) above 30% within replicates (this was the case for about one in four PSMs, taking about 2–3 min per PSM). The quantitation results were then exported using the Report Perspective option in Spectronaut.

To increase the confidence in our quantitation results and to simplify the evaluation of the data set, for each dilution series we only included residue pairs that were quantifiable across the full set of respective triplicates. Using “match between runs” in Spectronaut enabled peptides to be quantified across replica even without being initially detected in every single replica. In the 1 \times sample, this yielded 292 (70%) quantified URPs out of 414 identified URPs. The same injection amount (1.5 μ g) of HSA, albeit alone and not in mixture with six other proteins, analyzed by DDA led to 90 (95%) of 94 identified URPs being quantified across triplicate injections of a dilution series (0.1 \times , 0.3 \times , 0.5 \times , 0.9 \times , 1 \times). This means that DDA produced a higher quantified-to-identified ratio relative to DIA (Fig. 3A), at least when relying on the automated quantitation in Skyline. In how far this quantification is reliable will be investigated below. Interestingly, upon adding the foreign SEC data set (121 URPs) to the library, 66 unique residue pairs could be additionally quantified (Fig. 3C). The success rate of quantification was lower for this data (55%). Nevertheless, DIA allowed cross-links that had not been identified from a very extensive set of DDA acquisitions during library generation to be quantified. The overall success rate was 67% (358 quantified in at least one set of triplicates out of 535 URPs in the combined library). This relative proportions of URPs across the individual dilution samples were: 62% (1 \times), 62% (0.9 \times), 58% (0.7 \times), 54% (0.5 \times), 47% (0.3 \times), and 35% (0.1 \times). Peak area variation is represented using a coefficient of variation (CV) for each set of triplicates in the dilution experiment (Fig. 4A). The higher a CV value, the more variation was introduced during acquisition between peak areas of all replica pertaining to conditions. As one would expect, the lowest CV value is found for 1 \times dilution (CV: 10%). The CV value of the other dilutions ranges from 12 to 15% (0.1: 15%, 0.3: 12%, 0.5: 13%, 0.7: 12%, 0.9: 15%). This compares favorably with DDA, where only a single protein (HSA) was analyzed with a CV value of 66% for the 1 \times dilution (Fig. 3B). CVs of the other dilutions range from 42–76% (0.1: 42%, 0.3: 50%, 0.5: 76%, 0.9: 68%) (Fig. 4B). It compares also favorably to a previous DDA study using HSA, same cross-linker chemistry and manual curation of the whole data set, which resulted in a CV of 14% for the 1 \times (undiluted) sample (35). The reliability of DIA is further underpinned considering that a higher sample

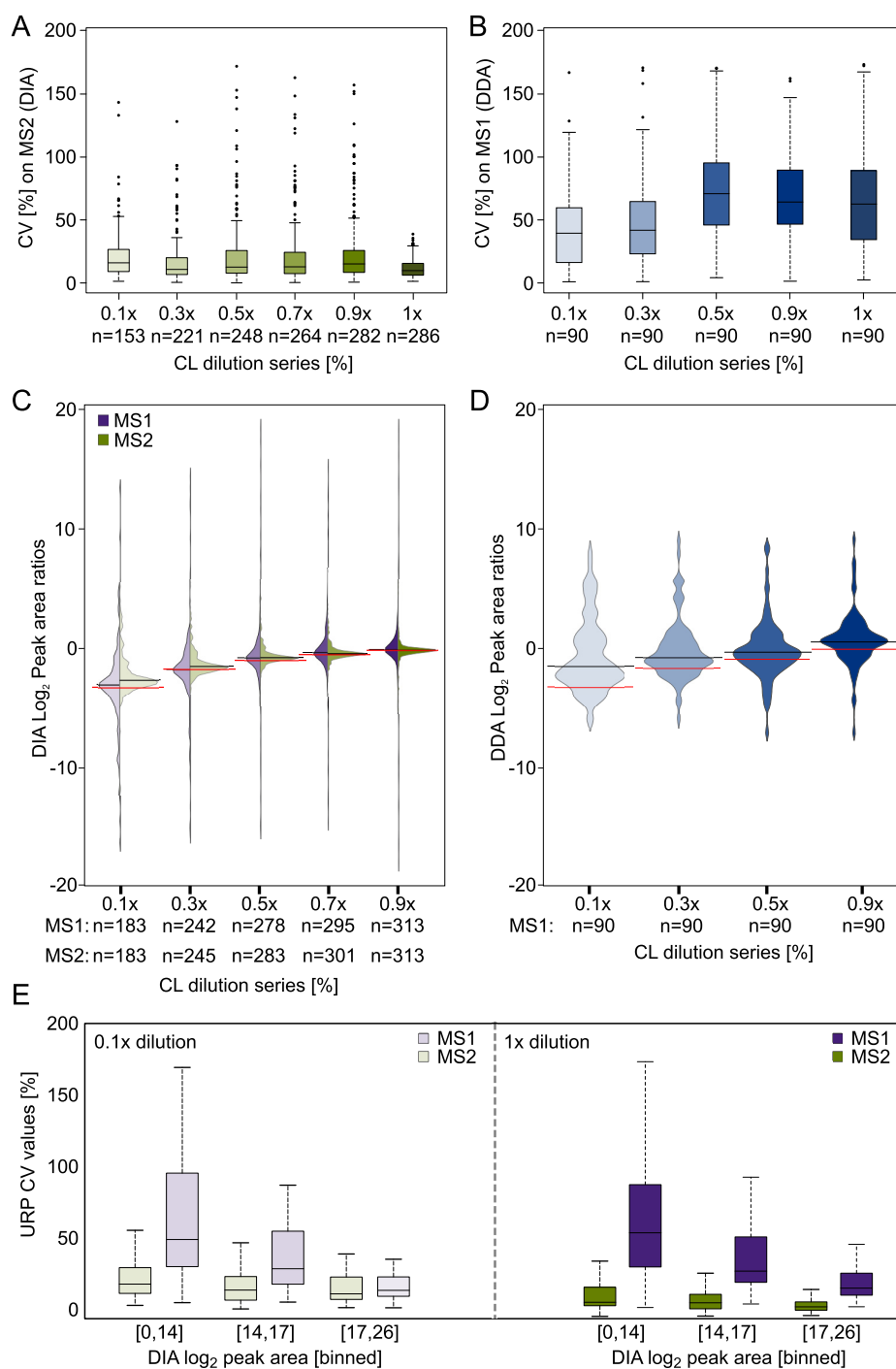


FIG. 4. Reproducibility of quantified unique residue pairs comparing data-independent and data-dependent acquisition. *A*, Coefficient of variation (CV) within triplicates on MS2 level from median peak areas in % for each dilution step after quantitation (DIA), showing the reproducibility of label-free quantitation of peak areas. Box plot whiskers extend 1.5 times the interquartile range. *B*, Coefficient of variation (CV) within triplicates on MS1 level from the DDA analysis, median peak areas in % for each dilution step. Box plot whiskers extend 1.5 times the interquartile range. *C*, Log₂ peak area ratios of each dilution step, showing precision of mixing (black line) versus expected ratios (red line) on MS2 (green) and MS1 (purple) level. *D*, Log₂ peak area ratios of each dilution step of DDA analysis, showing precision of mixing (black line) versus expected ratios (red line) on MS1 level (blue). *E*, CV from binned log₂ peak areas in % of the 0.1x and 1x dilution (DIA), showing anticorrelation between residue pair peak areas and CV values (MS1: purple, MS2: green).

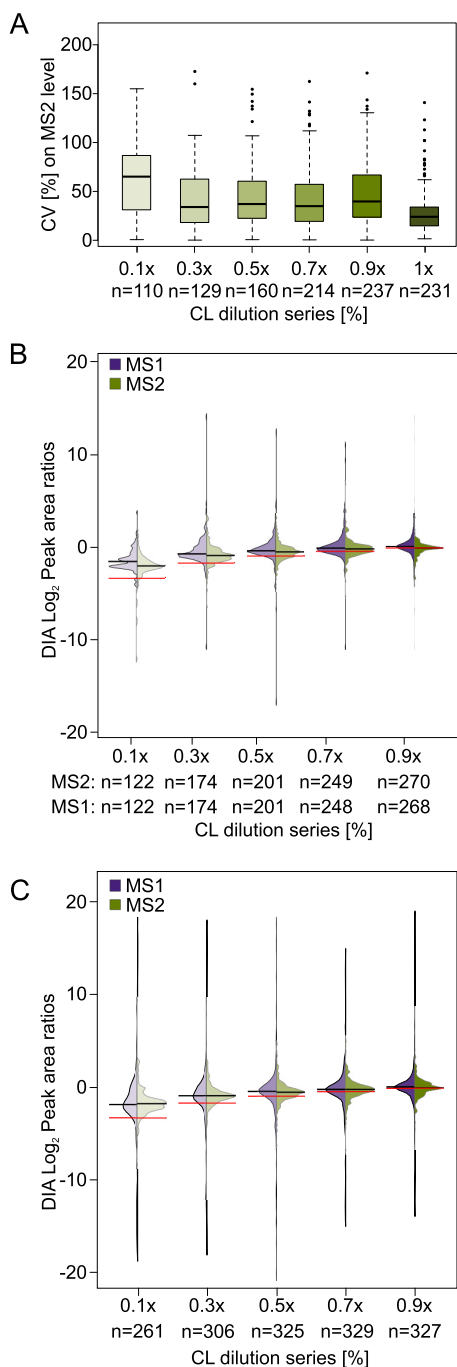


FIG. 5. Reproducibility of quantitation of unique residue pairs in a dilution series in a matrix of tryptic *E. coli* lysate and using shortened acquisition time. A, Coefficient of variation (CV) on MS2 level from median peak areas in % for each dilution step after quantitation, showing the reproducibility of label-free quantitation of peak areas. Box plot whiskers extend 1.5 times the interquartile range. B, Log₂ peak area ratios of each dilution step, showing precision of mixing (black line) versus expected ratios (red line) on MS2 (green) and MS1 (purple) level. C, Log₂ peak area ratios of each dilution step, showing precision of mixing (black line) versus expected ratios (red line) on MS2 (green) and MS1 (purple) level using interference correction option in Spectronaut and a *E. coli* background library.

complexity increases the dynamic range problem and therefore impacts quantitation negatively.

Although CV values are in the same range for each DIA dilution experiment, an anticorrelation within each experiment between residue pair peak areas and CV values are clearly shown for undiluted as well as 0.1× dilution samples (Fig. 4E). This was also previously shown for DDA cross-linking data (35). This is consistent with the expectation that low intense features are less accurately quantified.

We then assessed how well ratios between samples could be determined in our dilution series. Based on MS2 peak areas, the dilution series could be clearly revealed. However, at high dilutions, the apparent dilution was smaller than the true dilution, for example, 0.1× appeared as only 0.137× (Fig. 4C). This ratio compression is presumably related to low MS2 peak intensities and the contribution of noise. Changing to MS1 level, which is characterized by higher signal intensities and higher S/N ratio, the apparent dilutions matched the actual dilutions in this data set more closely (0.1× looked like 0.104×). Contrary to DIA, the DDA dilution series matches poorly the expected ratios, even the 0.9x dilution shows clearly a ratio compression (Fig. 4D). This agrees with the high conditional CV values, which represent less reproducibility within each triplicate of each dilution experiment.

Label-free Quantitation of Cross-linked Peptides in a Complex Background—Cross-linked peptides are generally of low abundance because of substoichiometric cross-linking and often, multiple cross-link options for individual residues. This makes the detection of cross-linked peptides especially challenging as sample complexity increases. To probe the limits of our DIA-QCLMS workflow, we used tryptic *E. coli* lysate as a complex matrix, added to our dilution series at a 1:1 wt/wt ratio for the 1× dilution and respectively in 10-fold excess for our 0.1× dilution sample. An additional challenge to using the same DIA method as for the original dilution series was that the gradient time was shortened from 150 min to 85 min resulting in 7 (MS1) and 2 (MS2) data points per peak on average. As one would expect, this reduced the success rate at which URPs could be quantified across all samples (58%, down from 67% across 18 samples). CV values also deteriorated to 24% for 1:1 comparisons and 34–64% for the other dilution steps (Fig. 5A). To determine whether changes in abundance of cross-linked residue pairs were still distinguishable, MS1 and MS2 peak area ratios were plotted as log₂ (Fig. 5B). MS1 and MS2 peak areas are very similar but differ notably in their expected ratios (red lines in violin plot), likely as a result of interferences from the increased sample complexity. This would also explain the higher CV values. Increasing complexity of samples therefore poses a challenge to quantitation success. Another explanation could be an interference effect caused by co-eluting precursors from the *E. coli* background (69). Adding a background library to our cross-link library and enabling interference correction in Spectronaut, shifted the MS2 peak area

distribution of cross-linked peptides toward low intense peak areas (supplemental Fig. S1f), without differences in MS1 or CV values compared with disabling interference correction (supplemental Fig. S1h, S1g). Although this distribution shift might have led to a closer match of peak area ratios to the expected ratios, the effect of interference correction is not noticeable after summing up cross-link peptides to unique residue pairs (Fig. 5C). We wondered in how far summing up cross-linked peptides to residue pairs influences ratio distortion. Comparing data of the *E. coli* dilution series with and without the Top3 approach, often used in linear proteomics (70), showed an increase in ratio compression on MS1 (supplemental Fig. S2a) as well as MS2 level (supplemental Fig. S2b). In our case, using all available cross-linked peptides reduced ratio compression compared with using just the three most intense ones when quantifying residue pairs.

However, many cross-linked residue pairs could be quantified, and their abundances were distinguishable between different concentrations. Soon, the quantitation accuracy is likely to further improve and any dependence on manual data curation is likely to further decrease. For example, Spectronaut 12 has made progress on interference correction compared with the Spectronaut 11 version used here (see release notes). With enough awareness of the challenges connected to complex mixture analysis, it seems possible to detect differentially abundant cross-linked peptides in complex mixtures and hence to successfully conduct DIA-QCLMS under such conditions.

CONCLUSION

Adapting Spectronaut for QCLMS analyses has extended the efforts of our laboratory to expand established proteomic quantitation software to cross-linking data, as done previously with MaxQuant (71) and Skyline (35), following initial proof-of-principle tests for QCLMS (24). Biognosys has added cross-linking data to the set of experiments that are automatically tested in each weekly build of Spectronaut to sustain optimal support for cross-linked data in Spectronaut in the future. The high accuracy that could be achieved, and especially the low CV at 1:1, suggest that even small changes in protein states could be picked up by QCLMS. DIA and Spectronaut significantly widen the scope of potential scientific applications of QCLMS and makes the analysis of structural states of large protein complexes or even cellular structures now appear possible.

DATA AVAILABILITY

The mass spectrometry raw files, peak lists and the result files from xiFDR, xiDIA-library and Spectronaut used in this study have been deposited to the ProteomeXchange Consortium via the PRIDE partner repository with the dataset identifier PXD011036 (<http://proteomecentral.proteomexchange.org/cgi/GetDataset?ID=PX011036>).

* This work was supported by the Wellcome Trust (103139, 108504), an Einstein Visiting Fellowship to Angela M. Gronenborn and the DFG (RA 2365/4-1). The Wellcome Trust Centre for Cell Biology is

supported by core funding from the Wellcome Trust (203149).

§ This article contains supplemental Figures. The authors O.M.B., and L.R. are employees of Biognosys AG (Zurich, Switzerland). Spectronaut is a trademark of Biognosys AG.

|| To whom correspondence should be addressed. E-mail: juri.rappsilber@tu-berlin.de.

Author contributions: F.M. and J.R. designed research; F.M. performed research; F.M. analyzed data; F.M. and J.R. wrote the paper; L.K. provided software tool (xiDIA-library) for this study; O.M.B. software developer of Spectronaut; L.R. cTO of Biognosys.

REFERENCES

1. Sinz, A. (2014) The advancement of chemical cross-linking and mass spectrometry for structural proteomics: from single proteins to protein interaction networks. *Expert Rev. Proteomics* **11**, 733–743
2. Liu, F., and Heck, A. J. R. (2015) Interrogating the architecture of protein assemblies and protein interaction networks by cross-linking mass spectrometry. *Curr. Opin. Struct. Biol.* **35**, 100–108
3. Leitner, A., Faini, M., Stengel, F., and Aebersold, R. (2016) Crosslinking and mass spectrometry: an integrated technology to understand the structure and function of molecular machines. *Trends Biochem. Sci.* **41**, 20–32
4. Schneider, M., Belsom, A., and Rappsilber, J. (2018) Protein tertiary structure by crosslinking/mass spectrometry. *Trends Biochem. Sci.* **43**, 157–169
5. Chavez, J. D., and Bruce, J. E. (2018) Chemical cross-linking with mass spectrometry: a tool for systems structural biology. *Curr. Opin. Chem. Biol.* **48**, 8–18
6. Chen, Z. A., Jawhari, A., Fischer, L., Buchen, C., Tahir, S., Kamenski, T., Rasmussen, M., Lariviere, L., Bukowski-Wills, J.-C., Nilges, M., Cramer, P., and Rappsilber, J. (2010) Architecture of the RNA polymerase II-TFIIF complex revealed by cross-linking and mass spectrometry. *EMBO J.* **29**, 717–726
7. Leitner, A., Reischl, R., Walzthoeni, T., Herzog, F., Bohn, S., Förster, F., and Aebersold, R. (2012) Expanding the chemical cross-linking toolbox by the use of multiple proteases and enrichment by size exclusion chromatography. *Mol. Cell. Proteomics* **11**, M111.014126
8. Debrunner, P. G., and Frauenfelder, H. (1982) Dynamics of Proteins. *Annu. Rev. Phys. Chem.* **33**, 283–299
9. Karplus, M. (1984) Dynamics of proteins. *Adv. Biophys.* **18**, 165–190
10. Chen, Z. A., and Rappsilber, J. (2018) Protein dynamics in solution by quantitative cross-linking mass spectrometry. *Trends Biochem. Sci.* **43**, 908–920
11. Huang, B. X. (2006) Interdomain conformational changes in akt activation revealed by chemical cross-linking and tandem mass spectrometry. *Mol. Cell. Proteomics* **5**, 1045–1053
12. Huang, B. X., and Kim, H.-Y. (2009) Probing Akt-inhibitor interaction by chemical cross-linking and mass spectrometry. *J. Am. Soc. Mass Spectrom.* **20**, 1504–1513
13. Chen, Z. A., Pellarin, R., Fischer, L., Sali, A., Nilges, M., Barlow, P. N., and Rappsilber, J. (2016) Structure of complement C3(H₂O) revealed by quantitative cross-linking mass spectrometry and modeling. *Mol. Cell. Proteomics* **15**, 2730–2743
14. Chen, Z., Fischer, L., Tahir, S., Bukowski-Wills, J.-C., Barlow, P., and Rappsilber, J. (2016) Quantitative cross-linking mass spectrometry reveals subtle protein conformational changes. *Wellcome Open Res.* **1**, 5
15. Herbert, A. P., Makou, E., Chen, Z. A., Kerr, H., Richards, A., Rappsilber, J., and Barlow, P. N. (2015) Complement Evasion Mediated by Enhancement of Captured Factor H: Implications for Protection of Self-Surfaces from Complement. *J. Immunol.* **195**, 4986–4998
16. Tomko, R. J., Taylor, D. W., Chen, Z. A., Wang, H. W., Rappsilber, J., and Hochstrasser, M. (2015) A single α helix drives extensive remodeling of the proteasome lid and completion of regulatory particle assembly. *Cell* **163**, 432–444
17. Schmidt, C., Zhou, M., Marriott, H., Morgner, N., Politis, A., and Robinson, C. V. (2013) Comparative cross-linking and mass spectrometry of an intact F-type ATPase suggest a role for phosphorylation. *Nat. Commun.* **4**, 1985
18. Yu, C., Mao, H., Novitsky, E. J., Tang, X., Rychnovsky, S. D., Zheng, N., and Huang, L. (2015) Gln40 deamidation blocks structural reconfiguration

- and activation of SCF ubiquitin ligase complex by Nedd8. *Nat. Commun.* **6**, 10053
19. Boelt, S. G., Norn, C., Rasmussen, M. I., André, I., Čiplyš, Slibinskas, E. R., Houen, G., and Højrup, P. (2016) Mapping the Ca(2+) induced structural change in calreticulin. *J. Proteomics* **142**, 138–148
 20. Beilsten-Edmands, V., Gordiyenko, Y., Kung, J. C., Mohammed, S., Schmidt, C., and Robinson, C. V. (2015) eIF2 interactions with initiator tRNA and eIF2B are regulated by post-translational modifications and conformational dynamics. *Cell Discov.* **1**, 15020
 21. Koehler, C., Sauter, P. F., Wawryszyn, M., Girona, G. E., Gupta, K., Landry, J. J. M., Fritz, M. H.-Y., Radic, K., Hoffmann, J.-E., Chen, Z. A., Zou, J., Tan, P. S., Galik, B., Junttila, S., Stolt-Bergner, P., Pruneri, G., Gyenesei, A., Schultz, C., Biskup, M. B., Besir, H., Benes, V., Rappsilber, J., Jechlinger, M., Korbek, J. O., Berger, I., Braese, S., and Lemke, E. A. (2016) Genetic code expansion for multiprotein complex engineering. *Nat. Methods* **13**, 997–1000
 22. Chavez, J. D., Schweppe, D. K., Eng, J. K., Zheng, C., Taipale, A., Zhang, Y., Takara, K., and Bruce, J. E. (2015) Quantitative interactome analysis reveals a chemoresistant edgotype. *Nat. Commun.* **6**, 7928
 23. Müller, D. R., Schindler, P., Towbin, H., Wirth, U., Voshol, H., Hoving, S., and Steinmetz, M. O. (2001) Isotope-tagged cross-linking reagents. A new tool in mass spectrometric protein interaction analysis. *Anal. Chem.* **73**, 1927–1934
 24. Fischer, L., Chen, Z. A., and Rappsilber, J. (2013) Quantitative cross-linking/mass spectrometry using isotope-labelled cross-linkers. *J. Proteomics* **88**, 120–128
 25. Walzthoeni, T., Joachimiak, L. A., Rosenberger, G., Röst, H. L., Malmström, L., Leitner, A., Frydman, J., and Aebersold, R. (2015) xTract: software for characterizing conformational changes of protein complexes by quantitative cross-linking mass spectrometry. *Nat. Methods* **12**, 1185–1190
 26. Kukacka, Z., Rosulek, M., Strohal, M., Kavan, D., and Novak, P. (2015) Mapping protein structural changes by quantitative cross-linking. *Methods* **89**, 112–120
 27. Zheng, Q., Zhang, H., Wu, S., and Chen, H. (2016) Probing protein 3D structures and conformational changes using electrochemistry-assisted isotope labeling cross-linking mass spectrometry. *J. Am. Soc. Mass Spectrom.* **27**, 864–875
 28. Tan, D., Li, Q., Zhang, M.-J., Liu, C., Ma, C., Zhang, P., Ding, Y.-H., Fan, S.-B., Tao, L., Yang, B., Li, X., Ma, S., Liu, J., Feng, B., Liu, X., Wang, H.-W., He, S.-M., Gao, N., Ye, K., Dong, M.-Q., and Lei, X. (2016) Trifunctional cross-linker for mapping protein-protein interaction networks and comparing protein conformational states. *eLife Sci.* **5**, e12509
 29. Schmidt, C., and Robinson, C. V. (2014) A comparative cross-linking strategy to probe conformational changes in protein complexes. *Nat. Protoc.* **9**, 2224–2236
 30. Ong, S.-E., Blagoev, B., Kratchmarova, I., Kristensen, D. B., Steen, H., Pandey, A., and Mann, M. (2002) Stable isotope labeling by amino acids in cell culture, SILAC, as a simple and accurate approach to expression proteomics. *Mol. Cell. Proteomics* **1**, 376–386
 31. Chavez, J. D., Schweppe, D. K., Eng, J. K., and Bruce, J. E. (2016) In vivo conformational dynamics of Hsp90 and its interactors. *Cell Chem. Biol.* **23**, 716–726
 32. Thompson, A., Schäfer, J., Kuhn, K., Kienle, S., Schwarz, J., Schmidt, G., Neumann, T., Johnstone, R., Mohammed, A. K. A., and Hamon, C. (2003) Tandem mass tags: a novel quantification strategy for comparative analysis of complex protein mixtures by MS/MS. *Anal. Chem.* **75**, 1895–1904
 33. Yu, C., Huszagh, A., Viner, R., Novitsky, E. J., Rychnovsky, S. D., and Huang, L. (2016) Developing a multiplexed quantitative cross-linking mass spectrometry platform for comparative structural analysis of protein complexes. *Anal. Chem.* **88**, 10301–10308
 34. Ross, P. L., Huang, Y. N., Marchese, J. N., Williamson, B., Parker, K., Hattan, S., Khainovski, N., Pillai, S., Dey, S., Daniels, S., Purkayastha, S., Juhasz, P., Martin, S., Bartlett-Jones, M., He, F., Jacobson, A., and Pappin, D. J. (2004) Multiplexed protein quantitation in *Saccharomyces cerevisiae* using amine-reactive isobaric tagging reagents. *Mol. Cell. Proteomics* **3**, 1154–1169
 35. Müller, F., Fischer, L., Chen, Z. A., Auchynnikava, T., and Rappsilber, J. (2018) On the reproducibility of label-free quantitative cross-linking mass spectrometry. *J. Am. Soc. Mass Spectrom.* **29**, 405–412
 36. Nahnsen, S., Bielow, C., Reinert, K., and Kohlbacher, O. (2013) Tools for label-free peptide quantification. *Mol. Cell. Proteomics* **12**, 549–556
 37. Arike, L., Valgepea, K., Peil, L., Nahku, R., Adamberg, K., and Vilu, R. (2012) Comparison and applications of label-free absolute proteome quantification methods on *Escherichia coli*. *J. Proteomics* **75**, 5437–5448
 38. Bensimon, A., Heck, A. J. R., and Aebersold, R. (2012) Mass spectrometry-based proteomics and network biology. *Annu. Rev. Biochem.* **81**, 379–405
 39. Gillet, L. C., Navarro, P., Tate, S., Röst, H., Selevsek, N., Reiter, L., Bonner, R., and Aebersold, R. (2012) Targeted data extraction of the MS/MS spectra generated by data-independent acquisition: a new concept for consistent and accurate proteome analysis. *Mol. Cell. Proteomics* **11**, O111.016717
 40. Hu, A., Noble, W. S., and Wolf-Yadlin, A. (2016) Technical advances in proteomics: new developments in data-independent acquisition. *F1000Res.* **5**, 419
 41. Shi, T., Su, D., Liu, T., Tang, K., Camp, D. G., 2nd, Qian, W. J., and Smith, R. D. (2012) Advancing the sensitivity of selected reaction monitoring-based targeted quantitative proteomics. *Proteomics* **12**, 1074–1092
 42. Lange, V., Picotti, P., Dorn, B., and Aebersold, R. (2008) Selected reaction monitoring for quantitative proteomics: a tutorial. *Mol. Syst. Biol.* **4**, 222
 43. Picotti, P., and Aebersold, R. (2012) Selected reaction monitoring-based proteomics: workflows, potential, pitfalls and future directions. *Nat. Methods* **9**, 555–566
 44. Gillette, M. A., and Carr, S. A. (2013) Quantitative analysis of peptides and proteins in biomedicine by targeted mass spectrometry. *Nat. Methods* **10**, 28–34
 45. Peterson, A. C., Russell, J. D., Bailey, D. J., Westphall, M. S., and Coon, J. J. (2012) Parallel reaction monitoring for high resolution and high mass accuracy quantitative, targeted proteomics. *Mol. Cell. Proteomics* **11**, 1475–1488
 46. Barysz, H., Kim, J. H., Chen, Z. A., Hudson, D. F., Rappsilber, J., Gerloff, D. L., and Earnshaw, W. C. (2015) Three-dimensional topology of the SMC2/SMC4 subcomplex from chicken condensin I revealed by cross-linking and molecular modelling. *Open Biol.* **5**, 150005
 47. Chavez, J. D., Eng, J. K., Schweppe, D. K., Cilia, M., Rivera, K., Zhong, X., Wu, X., Allen, T., Khurgel, M., Kumar, A., Lampropoulos, A., Larsson, M., Maity, S., Morozov, Y., Pathmasiri, W., Perez-Neut, M., Pineyro-Ruiz, C., Polina, E., Post, S., Rider, M., Tokmina-Roszyk, D., Tyson, K., Vieira Parrine Sant'Ana, D., and Bruce, J. E. (2016) A general method for targeted quantitative cross-linking mass spectrometry. *PLoS ONE* **11**, e0167547
 48. Bilbao, A., Varesio, E., Luban, J., Strambio-De-Castillia, C., Hopfgartner, G., Müller, M., and Lisacek, F. (2015) Processing strategies and software solutions for data-independent acquisition in mass spectrometry. *Proteomics* **15**, 964–980
 49. Bruderer, R., Sondermann, J., Tsou, C.-C., Barrantes-Freer, A., Stadelmann, C., Nesvizhskii, A. I., Schmidt, M., Reiter, L., and Gomez-Varela, D. (2017) New targeted approaches for the quantification of data-independent acquisition mass spectrometry. *Proteomics*, **17**
 50. Yu, C., and Huang, L. (2018) Cross-linking mass spectrometry: an emerging technology for interactomics and structural biology. *Anal. Chem.* **90**, 144–165
 51. Maiolica, A., Cittaro, D., Borsotti, D., Sennels, L., Ciferri, C., Tarricone, C., Musacchio, A., and Rappsilber, J. (2007) Structural analysis of multiprotein complexes by cross-linking, mass spectrometry, and database searching. *Mol. Cell. Proteomics* **6**, 2200–2211
 52. Rappsilber, J., Mann, M., and Ishihama, Y. (2007) Protocol for micro-purification, enrichment, pre-fractionation and storage of peptides for proteomics using StageTips. *Nat. Protoc.* **2**, 1896–1906
 53. Ishihama, Y., Rappsilber, J., and Mann, M. (2006) Modular stop and go extraction tips with stacked disks for parallel and multidimensional peptide fractionation in proteomics. *J. Proteome Res.* **5**, 988–994
 54. Rappsilber, J., Ishihama, Y., and Mann, M. (2003) Stop and go extraction tips for matrix-assisted laser desorption/ionization, nanoelectrospray, and LC/MS sample pretreatment in proteomics. *Anal. Chem.* **75**, 663–670
 55. Kolbowksi, L., Mendes, M. L., and Rappsilber, J. (2017) Optimizing the parameters governing the fragmentation of cross-linked peptides in a tribrid mass spectrometer. *Anal. Chem.* **89**, 5311–5318
 56. Cox, J., and Mann, M. (2008) MaxQuant enables high peptide identification rates, individualized p.p.b.-range mass accuracies and proteome-wide protein quantification. *Nat. Biotechnol.* **26**, 1367–1372

57. Mendes, M. L., Fischer, L., Chen, Z. A., Barbon, M., O'Reilly, F. J., Bohlke-Schneider, M., Belsom, A., Dau, T., Combe, C. W., Graham, M., Eisele, M. R., Baumeister, W., Speck, C., and Rappsilber, J. (2018) An integrated workflow for cross-linking mass spectrometry. *bioRxiv*, **355396**
58. Fischer, L., and Rappsilber, J. (2017) Quirks of error estimation in cross-linking mass spectrometry. *anal. chem.* **89**, 3829–3833
59. Bruderer, R., Bernhardt, O. M., Gandhi, T., Miladinović, S. M., Cheng, L.-Y., Messner, S., Ehrenberger, T., Zanotelli, V., Butscheid, Y., Escher, C., Vitek, O., Rinner, O., and Reiter, L. (2015) Extending the limits of quantitative proteome profiling with data-independent acquisition and application to acetaminophen-treated three-dimensional liver microtissues. *Mol. Cell. Proteomics* **14**, 1400–1410
60. Bruderer, R., Bernhardt, O. M., Gandhi, T., Xuan, Y., Sondermann, J., Schmidt, M., Gomez-Varela, D., and Reiter, L. (2017) Optimization of experimental parameters in data-independent mass spectrometry significantly increases depth and reproducibility of results. *Mol. Cell. Proteomics* **16**, 2296–2309
61. Holman, J. D., Tabb, D. L., and Mallick, P. (2014) Employing ProteoWizard to convert raw mass spectrometry data. *Curr. Protoc. Bioinformatics*, 1–9
62. MacLean, B., Tomazela, D. M., Shulman, N., Chambers, M., Finney, G. L., Frewen, B., Kern, R., Tabb, D. L., Liebler, D. C., and MacCoss, M. J. (2010) Skyline: An open source document editor for creating and analyzing targeted proteomics experiments. *Bioinformatics* **26**, 966–968
63. Walzthoeni, T., Claassen, M., Leitner, A., Herzog, F., Bohn, S., Förster, F., Beck, M., and Aebersold, R. (2012) False discovery rate estimation for cross-linked peptides identified by mass spectrometry. *Nat. Methods* **9**, 901–903
64. Vizcaíno, J. A., Deutsch, E. W., Wang, R., Csordas, A., Reisinger, F., Ríos, D., Dianes, J. A., Sun, Z., Farrah, T., Bandeira, N., Binz, P.-A., Xenarios, I., Eisenacher, M., Mayer, G., Gatto, L., Campos, A., Chalkley, R. J., Kraus, H.-J., Albar, J. P., Martinez-Bartolomé, S., Apweiler, R., Omenn, G. S., Martens, L., Jones, A. R., and Hermjakob, H. (2014) ProteomeXchange provides globally coordinated proteomics data submission and dissemination. *Nat. Biotechnol.* **32**, 223–226
65. Vizcaíno, J. A., Csordas, A., Del-Toro, N., Dianes, J. A., Griss, J., Lavidas, I., Mayer, G., Perez-Riverol, Y., Reisinger, F., Ternent, T., Xu, Q. W., Wang, R., and Hermjakob, H. (2016) 2016 update of the PRIDE database and its related tools. *Nucleic Acids Res.* **44**, D447–D456
66. Rosenberger, G., Bludau, I., Schmitt, U., Heusel, M., Hunter, C. L., Liu, Y., MacCoss, M. J., MacLean, B. X., Nesvizhskii, A. I., Pedrioli, P. G. A., Reiter, L., Röst, H. L., Tate, S., Ting, Y. S., Collins, B. C., and Aebersold, R. (2017) Statistical control of peptide and protein error rates in large-scale targeted data-independent acquisition analyses. *Nat. Methods* **14**, 921–927
67. Käll, L., Storey, J. D., MacCoss, M. J., and Noble, W. S. (2008) Posterior error probabilities and false discovery rates: two sides of the same coin. *J. Proteome Res.* **7**, 40–44
68. Reiter, L., Rinner, O., Picotti, P., Hüttenhain, R., Beck, M., Brusniak, M.-Y., Hengartner, M. O., and Aebersold, R. (2011) mProphet: automated data processing and statistical validation for large-scale SRM experiments. *Nat. Methods* **8**, 430–435
69. Ting, L., Rad, R., Gygi, S. P., and Haas, W. (2011) MS3 eliminates ratio distortion in isobaric multiplexed quantitative proteomics. *Nat. Methods* **8**, 937–940
70. Silva, J. C., Gorenstein, M. V., Li, G.-Z., Vissers, J. P. C., and Geromanos, S. J. (2006) Absolute quantification of proteins by LCMSE: a virtue of parallel MS acquisition. *Mol. Cell. Proteomics* **5**, 144–156
71. Chen, Z. A., Fischer, L., Cox, J., and Rappsilber, J. (2016) Quantitative cross-linking mass spectrometry using isotope-labeled cross-linkers and MaxQuant. *Mol. Cell. Proteomics* **15**, 2769–2778